Structures 57 (2023) 105224

Contents lists available at ScienceDirect

Structures

journal homepage: www.elsevier.com/locate/structures

Minimum design bending moment for systems of equivalent stiffness

Alexandre de Macêdo Wahrhaftig [a,*], Vagelis Plevris [b], Barhm Abdullah Mohamad [c], Dagoberto Lopes Pereira [d]

[a] Federal University of Bahia, Polytechnic School, Department of Construction and Structures, Rua Aristides Novís, 02, 5° andar, Federação, Salvador BA, Brazil
[b] Qatar University, Department of Civil and Environmental Engineering, P.O. Box: 2713, Doha, Qatar
[c] Erbil Polytechnic University, Koya Technical Institute, Department of Petroleum Technology, 44001 Erbil, Iraq
[d] Federal Institute of Education, Science and Technology of Bahia, R. Emídio dos Santos, s/n - Barbalho, Salvador BA, Brazil

ARTICLE INFO

Keywords:
Minimum design moment
Equivalent stiffness
Buckling
Rheological behavior
Reinforced concrete column
Rayleigh method

ABSTRACT

In this article, the minimum design bending moment of concrete slender columns is studied by assuming a system of equivalent stiffness. For concrete structural parts such as slender columns, their stiffness is dependent on the loading, originated from lumped and distributed masses, and the rheological behavior of the material. The latter alters the concrete's modulus of elasticity, introducing changes over time. Basically, the desired transformation is from a one-dimensional non-prismatic system to another prismatic one which exhibits an equivalent bending stiffness. As the bending stiffness changes due to the change of the problem's independent variables, the geometric characteristics of the transformed system reflect the same dependence as the original system. This implies changes in the minimum design moment since it is linked to the dimensions of the equivalent section. To assess the hypothesis proposed, a numerical simulation is conducted over a real structural system using a vertical loading ranging from zero up to the critical buckling force, taking into account the change in the modulus of deformation of concrete and assuming a certain level of cracking of the material. The results obtained showed that the strategy of using a system of equivalent stiffness simplifies the analysis of non-prismatic elements because the problem is reduced to a prismatic element of equivalent properties. Besides that, due to the incorporation of the concrete creep in the problem, the maximum moment obtained in the equivalent system needs to be multiplied by a factor of 2.94 in order to equal the maximum moment occurring in the original system.

1. Introduction

The solution of problems related to one-dimensional structural elements with variable geometry, i.e., non-prismatic bars, usually involves the definition of an element with equivalent stiffness. Non-uniform members such as stepped, tapered columns are being widely adopted to solve practical problems because they can reduce the self-weight and the cost of the structure [1]. In structures without initial imperfections, considering special loading cases, stability loss may occur due to bifurcation of equilibrium or buckling. This is the case for columns loaded axially and subjected to the concomitant action of concentrated loads and distributed forces along their axis, including their self-weight. For civil structures, usually, the vertical forces, either concentrated or distributed, are derived from the presence of masses, concentrated or distributed, in the gravitational field of the earth. In particular, in the case of concrete, structural parts such as slender columns have stiffness that depends on the load, in terms of the existing masses, and on the rheological behavior of the concrete, associated with creep. The latter introduces changes in the Young's modulus of the material, causing its value to vary over time.

Creep is a phenomenon that originates in the viscoelastic behavior of concrete, which accounts for increasing strain over time [2], even under constant stress [3]. Modern high-strength concretes also exhibit this behavior [4–5]. Creep changes the columns' stiffness, and for that reason it needs to be taken into account in the determination of the critical buckling load. One of the factors that contributes most to its occurrence is the relative air humidity [6–8], which depends on the climate and local conditions [9]. In the case of concrete structures, the presence of cracks further aggravates the problem by reducing the area moment of inertia of the cross-sections and at the same time opening passages for the ingress of water [10]. Generally, a slender reinforced concrete (RC) column can reach an ultimate limit state, which is

* Corresponding author.
E-mail addresses: alixa@ufba.br (A. de Macêdo Wahrhaftig), vplevris@qu.edu.qa (V. Plevris), barhm.mohamad@epu.edu.iq (B. Abdullah Mohamad), dagoberto.pereira@ifba.edu.br (D. Lopes Pereira).

https://doi.org/10.1016/j.istruc.2023.105224
Received 22 May 2023; Received in revised form 19 August 2023; Accepted 10 September 2023
Available online 16 September 2023

characterized by the loss of stability, without exhausting the bearing capacity of its cross-sections [11].

For slender reinforced concrete columns, the structural stiffness must be expressed as a function of two variables, forcing adjustments to the stiffness of the equivalent system when the values of these two parameters vary. Basically, the desired transformation is from a non-prismatic system, with stiffness depending on the applied masses (forces) and time, into a prismatic one, with equivalent bending stiffness. As the bending stiffness changes due to the change of the problem's independent variables, the geometric part of the bending stiffness product starts to reflect the same dependence on the structural stiffness. This implies changes in the minimum design moment, since it is linked to the dimensions of the cross-section of the equivalent system.

The concept of equivalent stiffness, as a rule, is an effective mathematical alternative for buckling analysis of non-uniform parts and/or systems of complex geometry [12–14]. The use of this concept can simplify the analysis of structural engineering problems involving composites [15–16], sections constituted by orthotropic material [17], and problems with geometric nonlinearities such as stretched cables [18]. It can also be used in dynamics to establish an equivalent mechanical model to calculate the first period of vibration of a tuned liquid damper [19], or to determine the capacity curve of a low-rise building in a nonlinear static analysis conducted through an equivalent single degree of freedom (SDOF) model to account for earthquake effects [20]. Equivalent systems of constant stiffness were also used to reduce the mathematical complexity variables of plate problems, allowing the extraction of a closed-form equation capable of solving elastic or inelastic systems [21].

In turn, the minimum design moment concept arises from the necessity of covering uncertainty regarding the normal force application point [22]. This does not account for the second-order effect, but can represent the maximum first-order moment for calculating the magnification factor for determining it [23]. When assuming the minimum design moment, most design codes frequently adopt a fixed eccentricity criterion for RC columns based on the dimensions of the analyzed cross-section. This procedure considers that the normal force acting on a section has a probability of occupying any point in the circle described by it [24]. So, for slender concrete columns the most important parameters of analysis are related to the magnitude of the axial force, first-order moments derived from the design eccentricities, creep, and the amount and distribution of reinforcement in the cross-sections [25]. As a result of these aspects, the structural analysis and assessment of an RC column must be performed as a combination of bending moments and axial force [26]. The solution method for this condition requires the employment of an interaction diagram, which should consider both the material and geometric parameters of the studied cross-section [27]. This procedure must be applied to several cross-sections of the column. In the case of the column being a non-prismatic member, the analytical effort required can be substantial.

Therefore, the creep effect has a significant impact on the minimum design bending moment of concrete columns because it produces additional longitudinal strains in relation to the considered element axis, which leads to transversal strains that alter the cross-section dimensions. When the dimensions of a cross-section are increased due to the concrete creep, the minimum design moment undergoes a proportional alteration at the same time. If a column has many cross-sections, the task of taking into account every section, one by one, requires much time and effort. This problem can be overcome by transforming the original non-prismatic system into an equivalent one, which simplifies the calculation process as the entire structure is taken into account instead of considering each section separately. The equivalent system is accounted through the structural stiffness. On the other hand, creep produces a change in the Young's modulus of concrete, reducing its value with time. This is reflected in both the ultimate and serviceability limit states. The former, for columns, can represent a loss of balance.

Taking this into consideration, the central objective of the present work is to evaluate the minimum design moment, in systems of equivalent stiffness, with concentrated vertical loading ranging from zero up to the critical buckling load, taking into account the change in the modulus of deformation of concrete, in time, and assuming a certain level of cracking in the material. The calculation of the critical buckling load was based on the concepts of structural dynamics, particularly those established first by Rayleigh in 1877 [28] for the vibration of systems without geometry variation, which have been adapted in this work for non-prismatic systems. The effect of creep and cracking in concrete was considered according to the requirements of ABNT NBR 6118 [29] of the Brazilian Association of Technical Standards (ABNT). Creep is also considered as in ACI-209R-08 [30] of the American Concrete Institute with compatible principles. This article therefore studies a design issue of slender RC columns, looking to preserve their structural safety and be of assistance to the practical engineer. Associated with the present issue, the calculation of structural stresses and strains can also be found in previous works [31–32].

2. Critical buckling load and structural stiffness

Euler in 1774 investigated analytically the problem of critical buckling load [33], and his studies were later complemented by Greenhill in 1881 [34], who included the self-weight in studying column stability by solving the Bessel function [35]. The self-weight of a column in compression is a decisive aspect for calculating the buckling load [36]. The postulations presented by Euler for the understanding of buckling were developed in the field of statics, starting from the analysis of the forces and moments induced in the central section of a bar with a perfectly vertical axis when considered laterally bent, whose solution was based on solving differential equations [37]. Euler considered that the column was in a flexed position because buckling is essentially a bending phenomenon, above all when observed from a statics point of view [38].

However, the study of buckling is directly related to the concept of the equilibrium of mechanical systems [39] and, for this reason, it also overlaps with the field of structural dynamics, where stiffness is a central part of the calculation process [40]. It is important to keep in mind that the material's behavior, given by its level of compressibility, directly influences the bearing capacity of slender columns since they can present buckling for continuous lateral deviation or snapping-through [41]. Temperature can also either potentiate or alleviate the buckling of RC columns because it produces internal forces due to the differences between the elastic proprieties of the concrete and reinforcement [42]. Despite the recent advances in material technology and the introduction of novel materials with superior properties, buckling remains an important research topic, such as in the cases of hyperelastic columns [43], and concrete armed with carbon nanotubes [44].

A slender RC column can be considered a continuous system that has infinite degrees of freedom (DOFs), subjected to axial compressive loads, including the self-weight. The system, from an equilibrium point of view, can be considered as a system that is still continuous but with a single DOF. In this way, the first buckling mode can be restricted to a configuration previously defined by an analytical function that is properly selected to represent it. From there, and based on the principle of the conservation of energy, the generalized properties of interest can be obtained, including the stiffness of the structural system.

Rayleigh applied the previous concept to the study of elements of prismatic form, considering a valid function throughout the domain. Since the method is based on energy conservation, it is suitable for both linear and non-linear problems. In this regard, the Rayleigh method or, as it became known later, the classical Rayleigh–Ritz method, was examined in comparison with the finite element formulation that has been considered as an efficient tool to solve non-linear problems of flexible bodies with the same level of accuracy [45]. For non-prismatic columns, the solution recommended by the Rayleigh method must be adapted to have its integrals resolved in the intervals defined in the

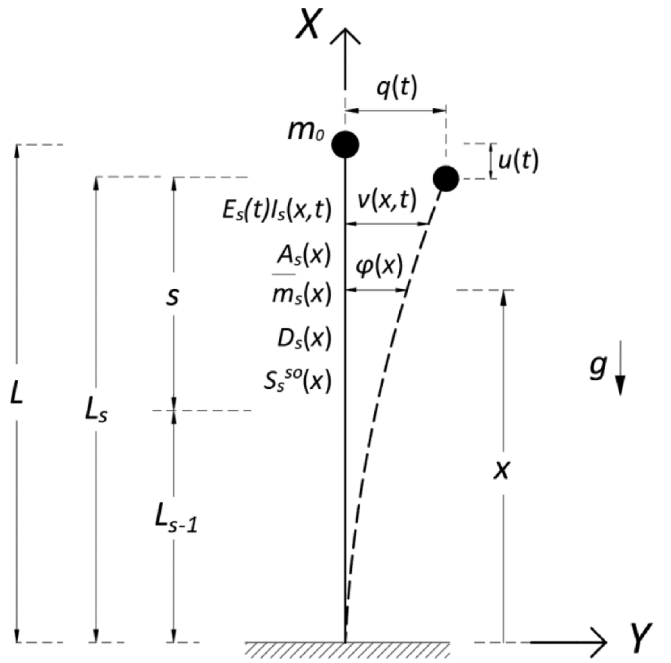

Fig. 1. Parameters of the non-prismatic source system.

analyzed geometry [46]. In correlated areas of study, Rayleigh's method was a precise tool to analyze composite anisotropic beams with arbitrary cross-section geometry [47], and to study the vibrations of a thin short cylindrical shell, including the viscoelastic behavior of its constituting material [48].

Fig. 1 depicts a model with a column clamped at the bottom part and free at its top end, a one-dimensional system contained in the plane *Y-X*, which represents an element that may have either constant or varying properties along its height. Such properties are the geometry, the modulus of elasticity (or viscoelasticity), and the material density. Under these conditions, the column is loaded with vertical forces due to the acceleration of gravity, g, which originates from the distributed mass, $\overline{m}_s(x)$, due to the structure's self-weight, and others that are added to it, and from the concentrated mass at the upper end, m_0, which will be defined in the imminence of the loss of stability by buckling, whose value, in terms of force, represents the capacity of the column in the vertical loading direction.

In the model of Fig. 1, t denotes time; $\varphi(x)$ is an analytical function describing the shape of the first buckling mode referred to *Y* direction; L is the length of the column; L_s and L_{s-1} are the locations at the upper and lower limits of a given segment s, whose length is calculated as the difference between these two positions; $E_s(t)$ is the viscoelastic modulus of the material; $I_s(x,t)$ is the area moment of inertia; $A_s(x)$ is the cross-sectional area; $D_s(x)$ is the external dimension; and $S_s^{So}(x)$ represents the lateral action of external springs. In this model, $q(t)$ is the generalized coordinate of the problem, located at the free end of the column, whose amplitude restricts the buckling movement to the proximity of its original straight configuration; $u(t)$ is the axial shortening due to lateral movement in the *X* direction; $v(x,t)$ is the function that gives the horizontal offset for each position x along the height, taken with respect to the shape function.

The equation $\varphi(x) = 1 - \cos(\pi x/(2L))$ constitutes a trigonometric function that describes the first buckling mode. The function is valid at any point in the structural domain, and it satisfies the problem's boundary conditions, i.e., $\varphi(0) = 0$ and $\varphi(L) = 1$. The distance variable x has its origin at the base of the system (where $x = 0$) and the positive x points upwards. That specific mathematical function reduces the system containing infinite degrees of freedom to a corresponding continuous one that contains a single DOF. The validity of the adopted equation for non-prismatic structures was adequately verified in comparison with finite element method results obtained computationally [49]. Applying the virtual work principle and its derivatives, the stiffnesses of interest can be obtained [50]. The conventional generalized elastic/viscoelastic stiffness portion is defined as:

$$K_0(t) = \sum_{s=1}^{n} k_{0s}(t) \text{ with}$$
$$k_{0s}(t) = \int_{L_{s-1}}^{L_s} E_s(t) I_s(x,t) \left(\frac{d^2\varphi(x)}{dx^2}\right)^2 dx \tag{1}$$

where s denotes the numbering of the structural segment and $E_s(t)$ is the time-varying modulus of elasticity of the material. If it is constant with time, it can simply be represented by E_s. $I_s(x,t)$ denotes the moment of inertia associated with the described buckling mode, a function of time in order to consider a possible homogenization of the section. If the material is viscoelastic and the segment is geometrically constant, the inertia is $I_s(t)$. If the modulus of elasticity is not a viscoelastic one, the inertia can be simply expressed as I_s for prismatic segments, or $I_s(x)$ for non-prismatic segments. $k_{0s}(t)$ is the term of the conventional stiffness varying in time, $K_0(t)$ is the total temporal part of the conventional stiffness and the number of existing segments in the analyzed geometry is denoted by n. The portion of the generalized geometric stiffness is presented as follows, as a function of the axial force, including the contribution of the self-weight:

$$K_g(m_0) = \sum_{s=1}^{n} k_{gs}(m_0), \text{ with} \tag{2}$$

$$k_{gs}(m_0) = \int_{L_{s-1}}^{L_s} \left[N_0(m_0) + \sum_{s+1}^{n} N_{s+1} + \overline{m}_s(x)(L_s - x)g \right] \left(\frac{d\varphi(x)}{dx}\right)^2 dx \text{ and } N_0(m_0) = m_0 g \tag{3}$$

where $K_g(m_0)$ is the structure's geometric stiffness, as shown in Eq. (2); $k_{gs}(m_0)$ is the fraction of the geometric stiffness of the segment s, defined by Eq. (3); $N_0(m_0)$ is the gravity force located at the upper end of the system. As can be seen, the portion of geometric stiffness depends on the mass m_0 located at the top of the column. In Eq. (3), N_s is the normal force from the distributed loading, obtained from:

$$N_s = \int_{L_{s-1}}^{L_s} \overline{m}_s(x) g dx, \text{ with } \overline{m}_s(x) = A_s(x)\gamma_s + \mu_s, \tag{4}$$

where $\overline{m}_s(x)$ is the distributed mass per unit length, $A_s(x)$ represents the geometrically variable area of the cross-section, γ_s is the material density and μ_s is an externally distributed mass added to the respective segment. If the cross-section has a constant area over the interval, this will simply be A_s and, as a result, the mass per unit length will also be constant. To consider the interaction with restoring forces in the equilibrium of the system, it is useful to represent them by a series of vertically distributed springs applied along the segment. This is an applicable approach in structural engineering because it is expected that the foundations respond elastically in service, even when subjected to extreme loading [51]. In this way, the contribution of the springs to the stiffness of the structure is expressed as:

$$K_{So} = \sum_{s=1}^{n} k_s, \text{ with } k_s = \int_{L_{s-1}}^{L_s} k_s^{so}(x)(\varphi(x))^2 dx \text{ and } k_s^{So}(x) = S_s^{So}(x) D_s(x), \tag{5}$$

where the parameter $k_s^{So}(x)$ depends on the geometry, $D_s(x)$, and an elastic property, $S_s^{So}(x)$, in each layer, s. Assuming the normal compression force as positive, the stiffness of the system is obtained as a function of two variables, time and the concentrated mass at the free end, as follows:

$$K(m_0, t) = K_0(t) - K_g(m_0) + K_{So} \tag{6}$$

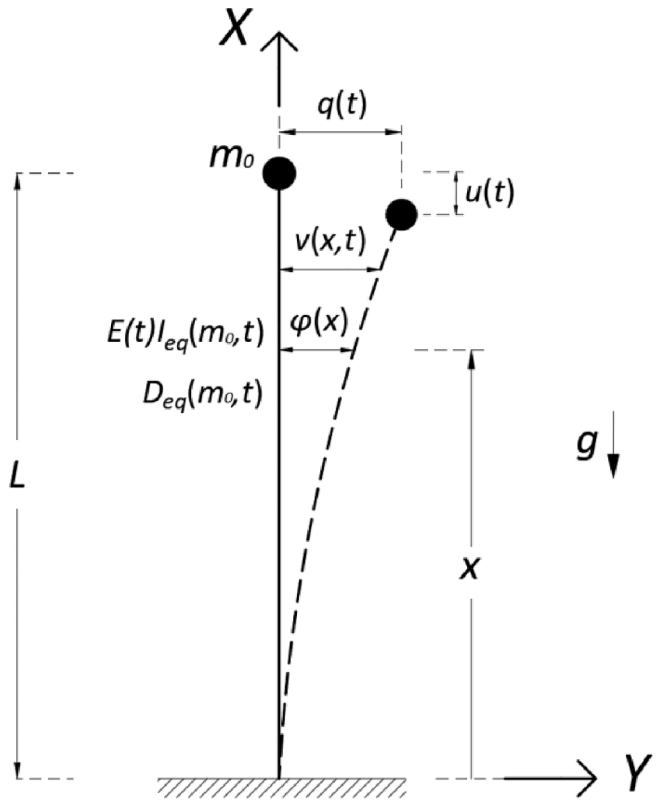

Fig. 2. Equivalent system parameters.

Considering the previous path and assuming a lumped mass, m_0, as the problem's independent variable, once the time instant, t, of interest is defined, the critical buckling load, $N_{cr}(t)$, can be calculated using the mathematical concept shown in Eq. (7), which defines the proximity of loss of equilibrium, that is, the vertical load capacity of the column, representing the moment when the column loses stiffness [52–53]. Therefore:

$$K(m_0,t)|_t = 0 \Rightarrow N_0(m_0) = N_{cr}(t) \tag{7}$$

3. Equivalent system and minimum design moment

The problem to be solved consists of the transformation of a non-prismatic system into a prismatic one of equivalent stiffness. For this, consider the model in Fig. 2, where $E(t)I_{eq}(m_0,t)$ and $D_{eq}(m_0,t)$ are the product of flexural stiffness and the section diameter of the equivalent system, where m_0 and t represent the mass at the top (free) end and time, respectively. The mathematical principles for the generalized coordinate $q(t)$, the axial shortening $u(t)$, the shape function $\varphi(x)$, and the acceleration of gravity, g, established for the non-prismatic source system, remain valid also in the equivalent system.

Under these conditions, the column bending stiffness is given by:

$$K(m_0,t) = \frac{3E(t)I_{eq}(m_0,t)}{L^3} \tag{8}$$

with $E(t)$ being the viscoelastic deformation modulus of the concrete, defined, for simple convenience, from the cross-sections subject to creep in the original system, being considered valid in the entire domain of the equivalent system. Therefore, it is credible to assume that:

$$I_{eq}(m_0,t) = \frac{K(m_0,t)L^3}{3E(t)} \tag{9}$$

Since the cross-section of the equivalent system is defined as having a circular shape, the equivalent diameter, $D_{eq}(m_0,t)$, can be written as:

$$D_{eq}(m_0,t) = \sqrt[4]{\frac{64I_{eq}(m_0,t)}{\pi}} \tag{10}$$

In turn, the minimum design moment, $M_{1dmin}(m_0,t)$, established in terms of the minimum design eccentricity, $e_{1dmin}(m_0,t)$, takes the following form:

$$M_{1dmin}(m_0,t) = N_0(m_0)e_{1dmin}(m_0,t) \tag{11}$$

with the minimum design eccentricity linked to the dimensions of the equivalent cross-section, as provided in ABNT NBR 6118 [29] and ACI R-318 [54], which can be expressed as follows:

$$e_{1dmin}(m_0,t) = 0.015m + 0.03D_{eq}(m_0,t) \tag{12}$$

Therefore, as can be seen, the cross-section dimensions of the equivalent system are also dependent on the mass at the free end and time, which induces a change in the minimum eccentricity and, consequently, in the minimum design moment of the equivalent section.

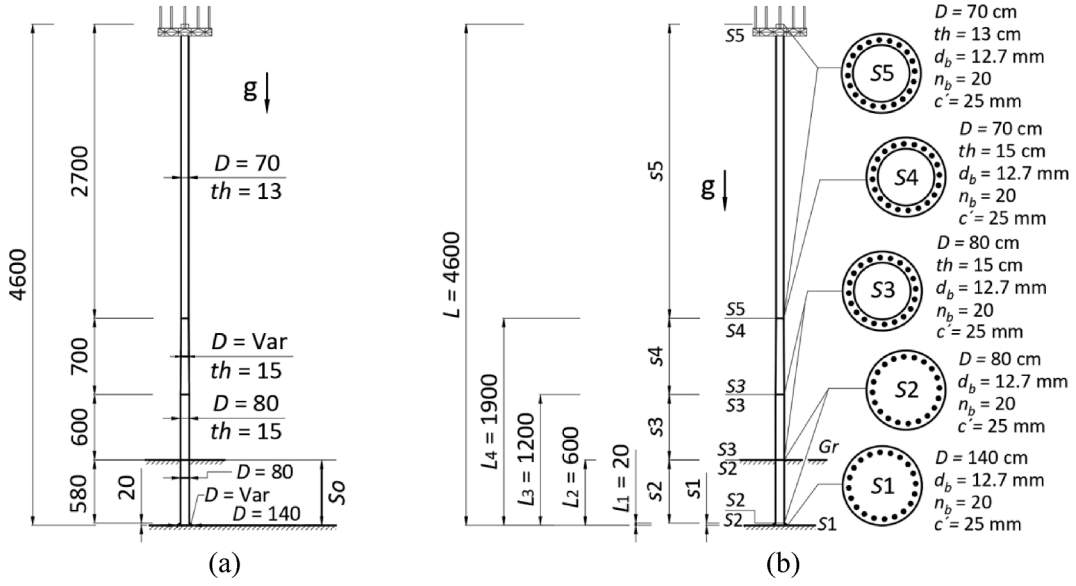

Fig. 3. Analyzed column: (a) geometry; (b) structural arrangement. Dimensions are in cm where not exclusively indicated.

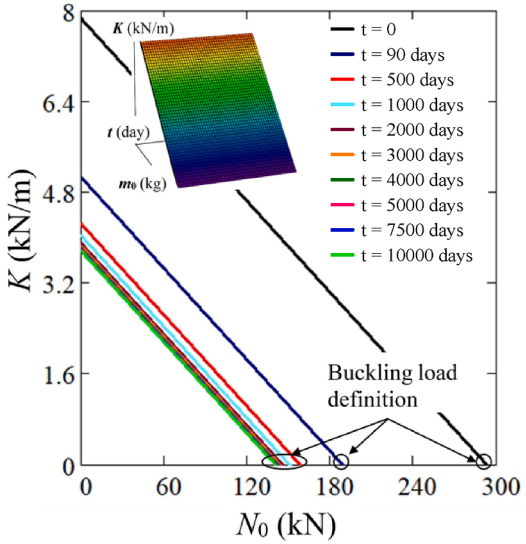

Time instant t (day)	Critical load N_{cr} (kN)	Variation δ (%)
0	293.4	-
90	189.2	35.5
500	158.6	16.2
1000	150.9	4.8
2000	145.9	3.3
3000	143.9	1.3
4000	142.9	0.7
5000	142.2	0.5
7500	141.3	0.6
10000	140.9	0.3
Δ (%) =	52	-

Fig. 4. Structural stiffness.

4. Assessment and numerical simulation

To evaluate the above concepts and determine the minimum design moment, a practical case study is considered. The structure is an extremely slender real pole made of RC, 46 m tall, including the 40 m superstructure, having a circular hollow section, and a 6 m deep foundation, of the caisson type. The foundation has a circular base (140 cm diameter), a height of 20 cm, and a circular shaft (80 cm diameter) with a length of 580 cm. All dimensions and structural arrangements are shown in Fig. 3, where g is the gravity acceleration pointing downwards; $S1$–$S5$ are the cross-sections, consecutively numbered from bottom to top (1 to 5); D is the external diameter; th indicates the thickness of the wall at the section; d_b is the diameter; n_b is the number of reinforcement bars; $\acute{c}$ is the concrete cover in the corresponding cross-sections; "Var" represents a variable section in the indicated segment; and So indicates the soil zone, that is, the buried part of the structure.

The concrete's initial tangent modulus defined for 28 days is 37566 MPa for the superstructure and 25044 MPa for the foundation, calculated according to the recommendations of ABNT NBR 6118 [29] considering the characteristic strengths of concrete, f_{ck}, equal to 45 MPa for the superstructure and 20 MPa for the foundation. Ordinarily, some equipment is attached to the top of the structure, which establishes a concentrated mass that affects the stability of the system related to buckling. Other devices or equipment may also be installed along the superstructure, which contributes an additional uniform mass of 40 kg/m. The soil–foundation interaction in the lateral direction is defined by an elastic constant equal to 2669 kN/m^3 in each layer. The cracking formation in the concrete was calculated by considering the moment of inertia reduced by a factor of 50% [29–30], considering that the flection dominates the work condition of the system.

The density of the RC was considered as 2600 kg/m^3 for the superstructure and 2500 kg/m^3 for the foundation part. Proper temporal homogenization factors were applied, which take into account the existence of the steel bars in the reinforcement by multiplying the nominal moment of inertia in each cross-section. Creep, due to the viscoelastic behavior of the concrete, was considered restricted to the superstructure, that is, to sections $S3$, $S4$, and $S5$, following the recommendations of the design code. Therefore, the total stiffness of the column, calculated with Eq. (6), can be found in Fig. 4.

The results for the stiffness and buckling critical load were produced

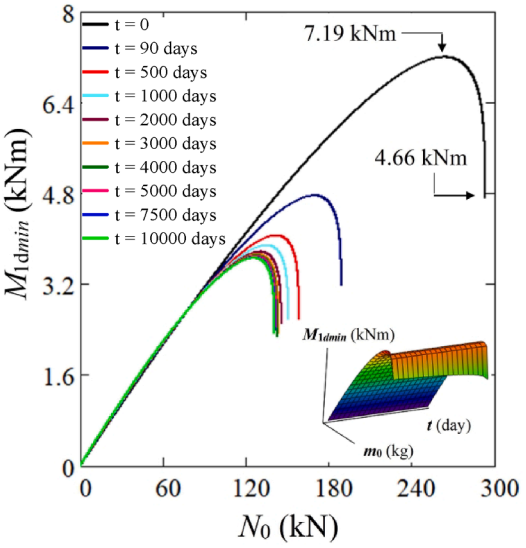

Time instant	Minimum moment				
t (day)	$0.9N_{cr}$ (kN)	δ (%)	N_{cr} (kN)	δ (%)	Δ (%)
0	7.19	-	4.66	-	35.2
90	4.76	33.8	2.92	37.3	38.7
500	4.05	14.9	2.53	13.4	37.5
1000	3.88	4.2	2.42	4.3	37.6
2000	3.77	2.8	2.28	5.8	39.5
3000	3.73	1.1	2.27	0.4	39.1
4000	3.70	0.8	2.28	-0.4	38.4
5000	3.69	0.3	2.27	0.4	38.5
7500	3.67	0.5	2.25	0.9	38.7
10000	3.66	0.3	2.21	1.8	39.6
Δ (%) =	49	-	53	Λ =	38.3

Δ = Absolute; δ = Relative; Λ = Average

Fig. 5. Minimum design bending moment of the equivalent system with the force at the top.

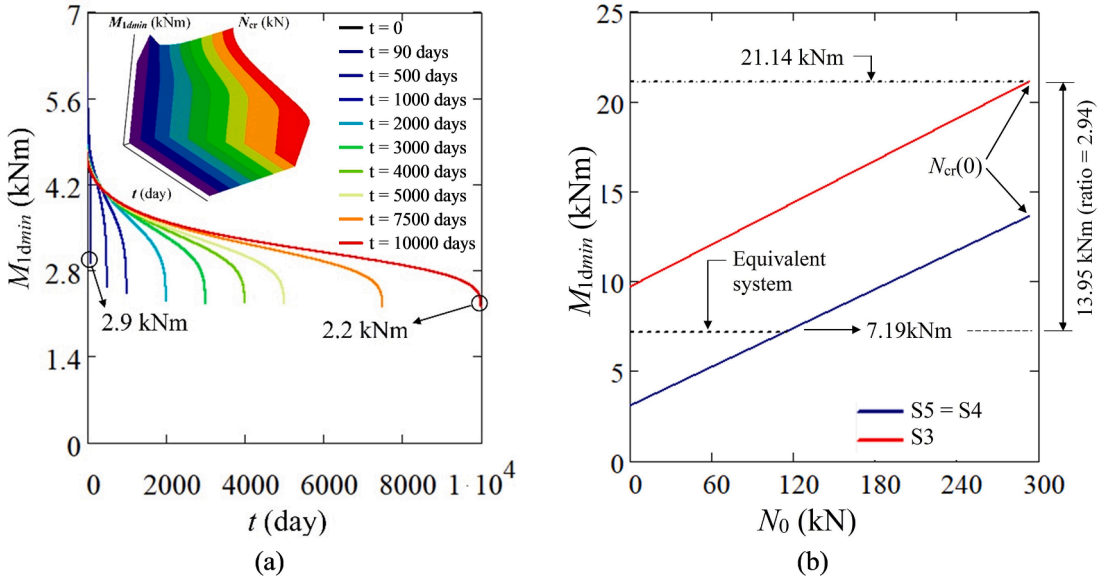

Fig. 6. (a) Minimum moment with time; (b) minimum moment of the original system with loading.

through the logical programing routine indicated in Appendix A, which was processed in Mathcad Software adopting incremental intervals for a mass of 1 kg, for a time of 1 day, and an expected tolerance of 10^{-6}. The processing considered different times within the period defined for the analysis, which was 10000 days after the structure had been loaded. After a careful checking, an initial value for the concentrated mass was adopted due to the fact that the processing in a regular computer is extremely time-consuming.

In Fig. 4 it is possible to observe the imminence of the loss of equilibrium for each instant of interest, with the definition of the corresponding vertical loading capacity of the system, established in terms of the nullity of stiffness, following the definition contained in Eq. (7). The table in Fig. 4 presents the results obtained for the critical buckling load, where δ and Δ indicate the variation for the current value and the total variation in the period; N_{cr} is the critical buckling load and t is the time at which the analysis takes place. The following were taken into account in the analyses: steel modulus of elasticity equal to 205 GPa, production of concrete considered standard conditions, relative humidity of the air 70%, and acceleration due to gravity equal to 9.807 m/s^2.

In the application of the concept of the equivalent system, the minimum design moment is a function of two variables, m_0 and t, such as the stiffness. The evaluation of the present problem can also be done by considering each independent variable in turn. With varying force at the top (free end) of the column, the results for various time instances can be seen in the graphs of Fig. 5.

In this case, the minimum moment of design of the equivalent system increases in value until the force at the top of the column reaches approximately 90% of the critical buckling load. At this position, the extreme value found is 7.19 kNm. From there, it starts to decrease until the column loading limit is reached, 4.66 kNm to the critical buckling load at the time of loading. The table in Fig. 5 presents the values for the minimum design moment to forces equal to $0.9N_{cr}$ and N_{cr} in their respective time instant. The average difference of the minimum moment related to these forces is around 38%. For both cases of force, the instant of 90 days is shown as that which produces the largest percentage decrement. This is associated with the standard creep model, which indicates that period as the most critical for the phenomenon to happen.

By setting the force at the top end at the value corresponding to the critical buckling load, the minimum design moment decreases with time, showing a more accentuated reduction, as a whole, for the first 3000 days of loading, as can be seen in Fig. 6(a). The smallest and largest reduction occur for the force at the top end when it is equivalent to the critical buckling load at the 90 days, with their values equal to 2.9 kNm and 2.2 kNm, respectively, a difference of 24%. It worth mentioning that the moment at the instant zero does not depend on time. Based on the same principles as Eq. (11), the minimum moment of the original system, considering the geometry of the cross-sections of interest ($S5$, $S4$ and $S3$), can be seen in Fig. 6(b). It is possible to observe that the highest value of 21.14 kNm is 2.94 times the maximum value found in the equivalent system. To calculate that, the forces due to the self-weight of

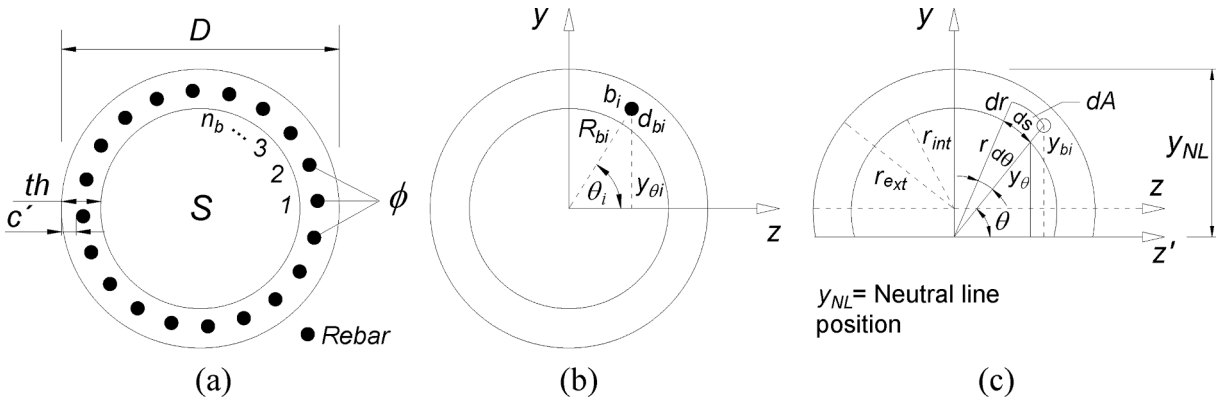

Fig. 7. Dimensions and reinforcement arrangement of a generic cross-section S.

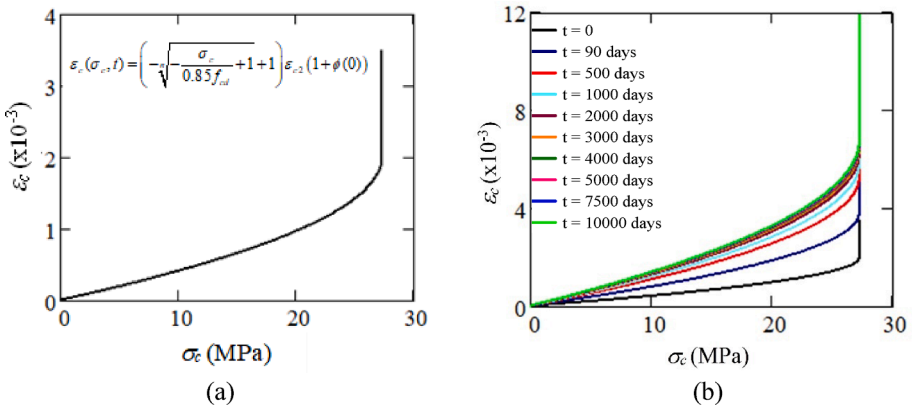

Fig. 8. Standard strain–stress diagram: (a) for $t = 0$; (b) for different time instants.

the above segments were considered according to Eq. (4).

For a first check of the structural safety in terms of bending moment, consider a generic section represented in Fig. 7(a) and (b), where n_b is the number of reinforcement rebars, *th* is the thickness of the wall, *c*' is the concrete covering, b_i indicates a generic rebar, *i*, of diameter d_{bi}, R_{bi} is the distance from the rebar central point to the section center, y_{0i} is the vertical distance between the rebar central line and the axis passing through the section center, and θ_i is the angle formed by R_{bi} and the horizontal axis *z*.

The resisting moment M_R of the section can be formulated considering θ as the independent variable of the problem, which varies from zero up to π under intervals $\Delta\theta = Sp/R_{bi}$ with $Sp = 2\pi R_{bi}/n_b$. So, the parcel resisted by the reinforcement according to the parameters in Fig. 7(b) is given by:

$$M_{st} = 2\left[\sum_{\theta} y(\theta)\frac{\pi d_{bi}^2}{4} f_{yd}\right], \text{ with}$$
$$y(\theta) = \sin(\theta)R_{bi} \text{ and } R_{bi} = \frac{D}{2} - c' - \frac{d_{bi}}{2} \tag{13}$$

where f_{yd} is the design yielding steel stress (250 MPa) divided by the steel safety coefficient (1.15). To compute the concrete participation, it is necessary to calculate the position of the neutral line y_{NL}, defined for the axis *z*', as shown in Fig. 7(c), where r_{ext} and r_{int} indicate, respectively, the external and internal radius of the cross-section, and all parameters such as *r*, θ, dr, dθ, ds, dA, y_0, y_{bi} are referred to the neutral line position, where *i* follows being a rebar indicator and the others say respect to the elementary concrete portion. For that, it is necessary to account for the strain produced at the same time by the bending moment and the axial force acting on the section. The first one, indicated as ε_M, is calculated through the curvature of the section, considering that:

$$\frac{1}{\rho} = \frac{M}{E(t)I}, \text{ and } \varepsilon_M = \frac{1}{\rho}\frac{D}{2}, \tag{14}$$

where ρ is the radius of curvature of the section, $E(t)$ is the viscoelastic modulus of concrete, *I* is the homogenized moment of inertia of the section, and *M* is the bending moment. On the other hand, there is the strain due to the axial force acting on the section. To calculate this last parcel, the equilibrium of forces and the condition of compatibility of strain must be analyzed as follows:

$$F_{st} = \frac{N/\gamma_a}{1 + \frac{1}{\eta(t)}\frac{1}{\omega}} \text{ and } F_c = \frac{N}{\gamma_a} - F_{st} \tag{15}$$

where F_{st} and F_c are the forces held by the reinforcement and concrete, respectively, γ_a is the safety factor of permanent actions, considered equal to 1.4, $\eta(t)$ is the relationship between the modulus of elasticity of the reinforcement steel, E_{st}, and that of the concrete, $E(t)$; and ω is the ratio of the mechanical area of reinforcement. So, the concrete stress, σ_c, is calculated considering the net area of concrete, A_c, by removing the total reinforcement area A_{st}:

$$\sigma_c = \frac{F_c}{A_c}, \text{ with } A_c = A_S - A_{st} \tag{16}$$

With that, by considering the strain–stress diagram of concrete in compression given by Fig. 8(a), obtained from the inverse relationship of the stress–strain normative curve, the parcel of the strain due to the axial force, ε_c, can be calculated in conformity with Eq. (17) for $t = 0$, due to the fact that at this time moment, the highest critical buckling load occurs. However, the present procedure can be done for an arbitrary moment of time, *t*, in conformity with the diagram of Fig. 8(b), which presents the strain curves considering the concrete creep for the different time instants assumed.

$$\varepsilon_c(\sigma_c, t) = \left(-\sqrt[n]{-\frac{\sigma_c}{0.85f_{cd}} + 1} + 1\right)\varepsilon_{c2}(1 + \phi(t)) \tag{17}$$

For the plot of the equation in Fig. 8, $n = 2$, and ε_{c2} is equal to 2.0×10^{-3}. The equation is valid for strain values between 0 and $3.5 \times 10^{-3}(1 + \phi(t))$. The calculation of the neutral line, which positions the axis *z*', must be done by the summation of Eqs. (14) and (17), encompassing the participation of both the normal and bending moment forces [55]. Considering that the internal and external radius of a generic section are:

$$r_{int} = \frac{D}{2} - th \text{ and } r_{ext} = \frac{D}{2} \tag{18}$$

and the resisting moment due to the compressed concrete considering Fig. 7(c) is:

$$M_c = \int_0^{\pi}\int_{r_{int}}^{y_{NL}} r^2\sin(\theta) f_{cd} dr d\theta - \int_0^{\pi}\int_{r_{ext}}^{y_{NL}} r^2\sin(\theta) f_{cd} dr d\theta - \sum_{\theta} y_{bi}(\theta)\frac{\pi d_{bi}^2}{4} f_{cd} \tag{19}$$

with

$$y_{st}(\theta) = (y_{NL} - c' - \frac{d_{bi}}{2})\sin(\theta) \tag{20}$$

where f_{cd} is the concrete design strength (45 MPa) divided by the concrete safety coefficient (1.40). The assessment of the structural safety can be done by analyzing the moment of resistance of the section *S*3 considering the contribution of both the reinforcement and the concrete. Therefore, assuming the definitions in Fig. 3, the total resisting bending moment of the mentioned section is 1285.05 kNm. This represents 60.78 and 178.73 times the minimum moment of the original and equivalent systems, respectively.

The moment of resistance, M_R, is given by summing Eqs (13) and (19). With that, it is possible to evaluate the minimum design moment in both the original and equivalent systems in comparison with the moment of resistance of section *S*3, considering the most critical buckling load and the self-weight of all the segments above it, as can be seen

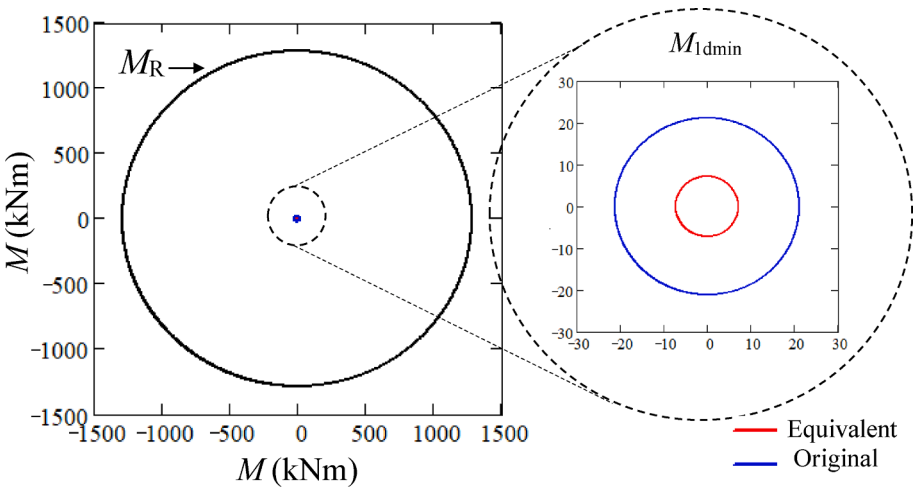

Fig. 9. Bending moments on section *S*3.

in Fig. 9.

5. Conclusions

The assessment of slender elements is performed taking into account both stability and resistance. A column is stable when its stiffness is preserved and is resistant when its cross-sections are capable of resisting the simultaneous action of two moments and the normal force. In that context, the assumption of a minimum design moment covers uncertainty regarding the real position of the normal force in each cross-section of the structure. If there are many different cross-sections to be considered, the design effort required can become extremely high. To overcome this problem, the adoption of an equivalent system is a feasible alternative.

In that context, the minimum design moment of a system of equivalent structural stiffness was evaluated. For this, the loading capacity of the original system, a slender column, made of RC, of varying section, was investigated using an analytical method based on the concepts of vibration of structural systems. All the necessary parameters were considered, such as the high slenderness of the column, the cracking formation, and the concrete creep. Because of creep, the analysis of a slender RC column must be done considering time.

Based on the analyses carried out, it can be concluded that:

For RC parts, the critical buckling force varies in time because the material's modulus of elasticity changes due to its viscoelastic behavior. For the analyzed case, the critical force calculated at the initial moment of loading and again at the end of the considered lifetime represented a 52% reduction in the vertical loading capacity of the column.

The structural safety of slender RC columns depends on time and loading. This dependency occurs because the structure's stiffness is composed of two parts, one which reflects the material's proprieties, and the other the intensity of the axial force (in terms of mass) acting on cross-sections. These dependencies are transposed also into the elaboration of the equivalent system.

In terms of resistance, once the equivalent system has been elaborated, and with the vertical loading accounted for, the analyst defines the analysis time and assesses the original system by using the transformed one, which can be easier to solve.

Considering the analyzed case, the minimum design moment of the equivalent system decreases by 24% with time since a certain loading level is set, but increases with the force at the top of the column when the instant of interest is established. This increase occurs until the loading reaches about 90% of the critical buckling load, when it begins to lessen, decreasing to the threshold value.

For the analyzed case, the maximum moment obtained in the equivalent system needs to be multiplied by the factor of 2.94 to equal the maximum moment occurring in the original system. The use of this coefficient preserves the structural safety. In this regard, the resisting moment of the critical cross-section was verified accordingly.

The adoption of an equivalent system to RC columns simplifies the analysis of practical problems and allows the assessment of these structures to be performed considering a certain time horizon.

The analysis of columns with other slenderness ratios and arrangements of sections are interesting topics for future research. Implications of the transformation of the geometric parameters of the cross-section of the transformed systems are also expected. Lateral forces acting on the structure and also producing bending are another point of interest.

Declaration of Competing Interest

The authors declare that they have no known competing financial interests or personal relationships that could have appeared to influence the work reported in this paper.

Acknowledgments

The first author thanks the National Council for Scientific and Technological Development (CNPq) for the support in the form of a research grant through the process 302494/2022-7, and the Coordination of Superior Level Staff Improvement (CAPES) for the support given through the process SIPAC/UFBA 23066.058305/2023-46.

Appendix A

Programing routine used to determine stiffness and buckling critical load.

1 INPUT:
2 INITIAL VALUE FOR m_0 AND t ($=t_0$).
3 VALUES FOR INCREMENTS Δm_0 AND Δt.
4 TOLERANCE FOR $K(m_0,t)$.
5 FINAL VALUE FOR t ($=t_f$).
6 PROCESSING:
7 CALCULATE $K(m_0,t)$.
8 VERIFY IF $K(m_0,t) <$ TOLERANCE.
9 IF IT IS NOT DO $m_0 = m_0 + \Delta m_0$.
10 THEN GO TO LINE 6.
11 IF IT IS STORAGE $N_{cr}(t) = m_0 g$.
12 VERIFY IF $t = t_f$.
13 IF IT IS NOT DO $m_0 =$ INITIAL VALUE FOR m_0 AND $t = t + \Delta t$.
14 THEN GO TO LINE 6.

```
    IF IT IS STOP.
CALCULATE M1dmin(m0,t) BASED ON K(m0,t).
OUTPUT.
DEFINE ARBRITARY TIME INSTANTS ti.
SUPPLY K(m0,ti), Ncr(ti) AND M1dmin(m0,ti).
PLOT K(m0,ti) WITH N0 = m0g.
PLOT M1dmin(m0,ti) WITH N0 = m0g.
PLOT M1dmin(m0i,t) FOR m0i = Ncr(ti)/g WITH t.
```

References

[1] Zhang H, Du L, Lu N. Exact stiffness matrix of multi-step columns and its application in non-uniform crane structure stability analysis. J Braz Soc Mech Sci Eng 2021;43:368. https://doi.org/10.1007/s40430-021-03077-3.

[2] Dummer A, Smaniotto S, Günter H. Experimental and numerical study on nonlinear basic and drying creep of normal strength concrete under uniaxial compression. Constr Build Mater 2023;362:129726. https://doi.org/10.1016/j.conbuildmat.2022.129726.

[3] Hong S-H, Choi J-S, Yuan T-F, Yoon Y-S. A review on concrete creep characteristics and its evaluation on high-strength lightweight concrete. J Mater Res Technol 2023;22:230–51. https://doi.org/10.1016/j.jmrt.2022.11.125.

[4] Shen D, Li C, Liu C, Li M, Kang J. Experimental investigations on early-age tensile creep of internally cured high strength concrete under different initial stress/strength ratios. Constr Build Mater 2020;265:120313. https://doi.org/10.1016/j.conbuildmat.2020.120313.

[5] Dias-da-Costa D, Julio ENBS. Modelling creep of high strength concrete. Comput Concr 2010;7(6):533–47. https://doi.org/10.12989/cac.2010.7.6.533.

[6] Magalhães KMM, Rebello da Fonseca Brasil RML, de Macêdo Wahrhaftig A, Siqueira GH, Bondarenko I, Neduzha L. Influence of Atmospheric Humidity on the Critical Buckling Load of Reinforced Concrete Columns. Int J Str Stab Dyn 2022;22(01).

[7] Ya W, Huang J, Liang S. Measurement and modeling concrete creep considering relative humidity effect. Mech Time-Depend Mater 2020;24:161–77. https://doi.org/10.1007/s11043-019-09414-3.

[8] Bouziadi F, Boulekbache B, Tahenni T, Haddi A, Hamrat M, Amziane S. Finite element analysis of steady-state uniaxial basic creep of high-performance concrete. J Build Eng 2022;52:104500. https://doi.org/10.1016/j.jobe.2022.104500.

[9] Sambito M, Severino A, Freni G, Neduzha L. A systematic review of the hydrological, environmental and durability performance of permeable pavement systems. Sustainability 2021;13:4509. https://doi.org/10.3390/su13084509.

[10] Shin KJ, Bae W, Choi S-W, Son MW, Lee KM. Parameters influencing water permeability coefficient of cracked concrete specimens. Constr Build Mater 2017;151:907–15. https://doi.org/10.1016/j.conbuildmat.2017.06.093.

[11] Ahmed B, Zerfu K, Agon EC, Wu C. Construction of uniaxial interaction diagram for slender reinforced concrete column based on nonlinear finite element analysis. Adv Civ Eng 2021;2021:1–10.

[12] Zhu X, Xiong C, Yin J, Yin D, Deng H. Equivalent stiffness prediction and global buckling analysis using refined analytical model of composite laminated box beam. Sci Eng Compos 2019;26(1):465–81. https://doi.org/10.1515/secm-2019-0030.

[13] Tao M-X, Li Z-A, Zhou Q-L, Xu L-Y. Analysis of equivalent flexural stiffness of steel–concrete composite beams in frame structures. Appl Sci 2021;11:10305. https://doi.org/10.3390/app112110305.

[14] Shadmehri F, Derisi B, Hoa SV. On bending stiffness of composite tubes. Compos Struct 2011;93(9):2173–9. https://doi.org/10.1016/j.compstruct.2011.03.002.

[15] Han S, Fan C, Zhou A, Ou J. Simplified implementation of equivalent and ductile performance for steel-FRP composite bars reinforced seawater sea-sand concrete beams: equal-stiffness design method. Eng Struct 2022;266:114590. https://doi.org/10.1016/j.engstruct.2022.114590.

[16] Kilimtzidis S, Kotzakolios A, Kostopoulos V. Efficient structural optimisation of composite materials aircraft wings. Compos Struct 2023;303:116268. https://doi.org/10.1016/j.compstruct.2022.116268.

[17] Yu Q, Xu H. A bran-new equivalent orthotropic-plate method for nonlinear bending of combined double bottom structure with variable stiffness. Compos Struct 2023;305:116547. https://doi.org/10.1016/j.compstruct.2022.116547.

[18] Xia GY, Cai CS. Equivalent stiffness method for nonlinear analysis of stay cables. Struct Eng Mech 2011;39(5):661–7. https://doi.org/10.12989/sem.2011.39.5.661.

[19] de Morais MVG, Lopez AAO, Martins JF, Pedroso LJ. Equivalent mechanical model of rectangular container attached to a pendulum compared to experimental data and analytical solution. J Braz Soc Mech Sci Eng 2020;42:143. https://doi.org/10.1007/s40430-020-2232-7.

[20] Malla N, Wijeyewickrema AC. Collapse assessment of low-rise reinforced concrete special moment resisting frame systems using a simplified method. Structures 2022;38:1–13. https://doi.org/10.1016/j.istruc.2022.01.076.

[21] Liu M-F, Chang T-P, Wang Y-H. Free vibration analysis of orthotropic rectangular plates with tapered varying thickness and Winkler spring foundation. Mech Based Des Struct Mach 2011;39(3):320–33. https://doi.org/10.1080/08905459308905187.

[22] Radwan M, Kövesdi B. Equivalent geometrical imperfections for local and global interaction buckling of welded square box section columns. Structures 2023;48:1403–19. https://doi.org/10.1016/j.istruc.2023.01.045.

[23] Saucha J, Rado J, Ivakovi C. The stability of an antenna column under the simultaneous action of its own weight and an effective load. Stroj Vestn-J Mech E 2017;47(1):4–14. https://www.sv-jme.eu/article/the-stability-of-an-antenna-column-under-the-simultaneous-action-of-its-own-weight-and-an-effective-load/.

[24] Jiang Y, Yang W. An approach based on theorem of total probability for reliability analysis of RC columns with random eccentricity. Struct Saf 2013;41:37–46. https://doi.org/10.1016/j.strusafe.2012.11.001.

[25] Marí AR, Hellesland J. Lower slenderness limits for rectangular reinforced concrete columns. *ASCE. J Struct Eng* 2005;131(1):85–95.

[26] C.Y. Lau, S.L. Chan, A.K.W. So, Biaxial bending design of arbitrarily shaped reinforced concrete column. *ACI Struct. J.* 90 (3) 269–278. https://doi.org/10.14359/4235.

[27] Kim JH, Lee SH, Paik I, Lee HS. Reliability assessment of reinforced concrete columns based on the P-M interaction diagram using AFOSM. Struct Saf 2015;55:70–9. https://doi.org/10.1016/j.strusafe.2015.03.003.

[28] Rayleigh JWS. Theory of sound. New York: Dover Publications; 1877. Reissued in 1945.

[29] Abnt. (Brazilian Association of Technical Standards), NBR 6118 - Design of Concrete Structures –. Rio de Janeiro Procedure 2014. https://www.abnt.org.br/assinatura-de-normas-tecnicas.

[30] ACI (American Concrete Institute), Prediction of creep, shrinkage, and temperature effects in concrete structures. ACI-209R-08, ACI Committee 209, Michigan, 2008. https://www.concrete.org/store/productdetail.aspx?ItemID=209208&Format=DOWNLOAD&Language=English&Units=US_AND_METRIC.

[31] Magalhães KMM, Wahrhaftig AM, Brasil RMLRF. Strain regime induced by axial compression in slender reinforced concrete columns using different mathematical approaches. Structures 2023;49:655–65. https://doi.org/10.1016/j.istruc.2023.01.148.

[32] Wahrhaftig AM, Magalhães KMM, Brasil RMLRF. Updating the bearing capacity, stresses, and strain for retrofitting reinforced concrete towers of the cellular and internet system. Mech Based Des Struct 2023;51(1):464–80. https://doi.org/10.1080/15397734.2020.1846559.

[33] L. Euler, De Curvis Elasticis, Additamentum I to his Methodus Inveniendi Lineas Curvas Maximi Minimive Proprietate Gaudentes, Lausanne and Geneva, 1744.

[34] Greenhill AG. Determination of the greatest height consistent with stability that a vertical pole or mast can be made, and the greatest height to which a tree of given proportions can grow. Proc Cambridge Philos Soc 1881;4:65–73. https://doi.org/10.1051/jphystap:018820010033701.

[35] Gere JM, Carter WO. Critical buckling load for tapered columns. ASCE J Struct Div 1963;88(3):1–11. https://www.steel.org.au/resources/elibrary/library/critical-buckling-loads-for-tapered-columns/.

[36] Wahrhaftig AM, Magalhães KMM, Brasil RMLRF, Murawski K. Evaluation of mathematical solutions for the determination of buckling of columns under self-weight. J Vib Eng Technol 2021;9:733–49. https://doi.org/10.1007/s42417-020-00258-7.

[37] Xiao BJ, Li XF. Exact solution of buckling load of axially exponentially graded columns and its approximation. Mech Res Commun 2019;101:103414. https://doi.org/10.1016/j.mechrescom.2019.103414.

[38] C.H. Yoo, S. Lee, Stability of Structures: Principles and Applications (2011). Oxford.

[39] Dražumerič R, Kosel F. Optimizing the geometry for the buckling of a bar. Stroj Vestn-J Mech E 2017;49(7–8):385–97. https://www.sv-jme.eu/article/optimizing-the-geometry-for-the-buckling-of-a-bar.

[40] I. Bondarenko, O. Lunys, L. Neduzha, R. Keršys, Dynamic track irregularities modeling when studying rolling stock dynamics. *Transport Means, Proceedings of the International Conference* (2019) 1014–1019. Palanga.

[41] Chen Y, Jin L. From continuous to snapping-back buckling: A post-buckling analysis for hyperelastic columns under axial compression. Int J Non Linear Mech 2020;125:103532. https://doi.org/10.1016/j.ijnonlinmec.2020.103532.

[42] Wahrhaftig AM, Magalhães KMM. Bifurcation analysis of columns of composite materials with thermal variation. Mater Res 2021;24:e20210266.

[43] Chen Y, Jin L. Snapping-back buckling of wide hyperelastic columns. Extreme Mech Lett 2020;34:100600. https://doi.org/10.1016/j.eml.2019.100600.

[44] Arani AJ, Kolahchi R. Buckling analysis of embedded concrete columns armed with carbon nanotubes. Comput Concr 2016;17(5):567–78. https://doi.org/10.12989/cac.2016.17.5.567.

[45] Jeong S, Yoo HH. Nonlinear structural analysis of a flexible multibody system using the classical Rayleigh-Ritz method. Int J Non Linear Mech 2019;110:69–80. https://doi.org/10.1016/j.ijnonlinmec.2019.01.011.

[46] Wahrhaftig AM, Magalhães KMM, Silva MA, Brasil RMLRF, Banerjee JR. Buckling and free vibration analysis of non-prismatic columns using optimized shape functions and Rayleigh method. Eur J Mech A Solids 2022;93:104543. https://doi.org/10.1016/j.euromechsol.2022.104543.

[47] Ghafari E, Rezaeepazhand J. Two-dimensional cross-sectional analysis of composite beams using Rayleigh-Ritz-based dimensional reduction method. Compos Struct 2017;184:872–82. https://doi.org/10.1016/j.compstruct.2017.10.049.

[48] Song X, Cao T, Gao P, Han Q. Vibration and damping analysis of cylindrical shell treated with viscoelastic damping materials under elastic boundary conditions via a unified Rayleigh-Ritz method. Int J Mech Sci 2020;165:105158. https://doi.org/10.1016/j.ijmecsci.2019.105158.

[49] Wahrhaftig AM. Analysis of the first modal shape using two case studies. Int J Comput Meth 2019;16(6):1840019. https://doi.org/10.1142/S0219876218400194.

[50] Fuchs MB. Structures and Their Analysis. In: Fuchs MB, editor. Structures and Their Analysis. Cham: Springer International Publishing; 2016. p. 53–66.

[51] Cucuzza R, Devillanova G, Aloísio A, Rosso MM, Marano GC. Analytical solutions for piles' lateral deformations: The nonlinear stiffness case. Int J Mech Sci 2022; 229:107505. https://doi.org/10.1016/j.ijmecsci.2022.107505.
[52] Wahrhaftig AM. Time-dependent analysis of slender, tapered reinforced concrete columns. Steel Compos Struct 2020;36(2). https://doi.org/10.12989/scs.2020.36.2.229.
[53] Wahrhaftig AM, Silva MA, Brasil RMLRF. Analytical determination of the vibration frequencies and buckling loads of slender reinforced concrete towers. Lat Am J Solids Struct 2019;16(5). https://doi.org/10.1590/1679-78255374.
[54] American Concrete Institute (ACI), Building code requirements for structural concrete, ACI 318-19. ACI Committee 318 (2019). Michigan. https://doi.org/10.14359/51716937.
[55] Su J, Liu B, Xing G, Ma Y, Huang J. Influence of beam-to-column linear stiffness ratio on failure mechanism of reinforced concrete moment-resisting frame structures. Adv Civ Eng 2020;2020:1–24.